Adaptive Exponential Integrate-and-Fire Model as an Effective Description of Neuronal Activity

Leonardo Hügens

l.lobatodiasleitehugens@students.uu.nl

6th June 2021

Abstract

In this project we study the Adaptive Exponential Integrate-and-Fire Model, with a focus in deriving analytical results about its subthreshold dynamics, complementing with some observations about how well this model can be fitted to real neuronal behaviors. We show there is a saddle-node bifurcation and a Andronov-Hopf bifurcation, deriving conditions for which each of them exist. We also argue that this model has enough expressive power to reproduce qualitatively real several types of *in vitro* neuron behavior.

1 Introduction

There is a clear interest among neuro-computing community in finding a model of a neuron which is simple enough to be efficiently simulated with computer programs, maybe even capable of providing precise results through analytical procedures, while being able to reproduce empirical observations. What happens in reality is that there is always a trade off between simulation efficiency and ability of the model to be fitted to data.

In this project, we analyze the Adaptive Exponential Integrate-and-Fire Model, a two dimensional model whose dynamical variables are the membrane potential V and an adaptation current w, which is given by the following system of differential equations:

$$\begin{cases} C\dot{V} &= I - g_{\mathrm{L}}\left(V - E_{\mathrm{L}}\right) + g_{\mathrm{L}}\Delta_{\mathrm{T}}\mathrm{e}^{(V-V_{\mathrm{T}})/\Delta_{\mathrm{T}}} - w \\ \tau_w\dot{w} &= a\left(V - E_{\mathrm{L}}\right) - w \end{cases} \tag{1}$$

It is intuitive to see that when the potential V gets high enough, the exponential term diverges, making the trajectory diverge, which is the spiking behavior in this model. It turns out to be both convenient from a simulation standpoint and interesting in the results it generates to include a reset procedure: when a spike occurs, the membrane potential V is instantaneously reset to

some value V_r and the adaptation current is increased:

$$\begin{cases} V & \to V_r \\ w & \to w + b \end{cases} \tag{2}$$

We will use analytical procedures to make precise statements about bifurcations in this model, and reflect on the relationship between behaviors generated by this model and real neuronal data. Unless stated otherwise, the constant values we're going to use to generate plots in this project are the one's obtain in [1] as the best fit, which are:

$$\begin{aligned} C &= 281\,\text{pF} \\ g_L &= 20\,\text{nS} \\ E_L &= -70.6\,\text{mV} \\ V_T &= -50.4\,\text{mV} \\ \Delta_T &= 2\,\text{mV} \\ \tau_w &= 144\,\text{ms} \\ a &= 4\,\text{nS} \\ b &= 0.0805\,\text{nA} \end{aligned} \tag{3}$$

2 Procedures and results in Brette and Gerstner [1]

For the analysis of the reproducibility of experimental data with the aEIF model, we will be following the paper *Adaptive Exponential Integrate-and-Fire Model as an Effective Description of Neuronal Activity* [1]. In this paper, this reproducibility was not studied against experimental data directly, but rather against another model, which was already shown to reproduce a lot of neuron behaviors well. This reference detailed model was a single-compartment model of a regular spiking pyramidal cell with voltage-dependent currents IM, INa, and IK (McCormick et al. 1993 [3]).

A quantitative comparison between the two models (aEIF and the detailed one) was made by using two measures of performance of aEIF. The first was M, which is the percentage of missing spikes (spikes were said to match if they are emitted withing 2 ms of each other), relative to the number of spikes in the detailed model. The second was Γ, the coincidence factor, as defined in Kistler et al. (1997) [2], which is

$$\Gamma = \frac{N_{\text{coinc}} - \langle N_{\text{coinc}} \rangle}{\frac{1}{2}\left(N_{\text{detailed}} + N_{\text{aeif}}\right)} \mathcal{N}^{-1}$$

where N_{detailed} and $N_{\text{aeif}}$are the total number of spikes emitted by either model, N_{coinc} is the number of spikes emitted by aEIF that happened within 2 ms of spikes emitted by the detailed model, $\langle N_{\text{coinc}} \rangle$ is the number of coincidences by chance relative to the total number of pikes produces by both models, and $\mathcal{N}$ is a normalization constant. If we define E as the percentage of

extra spikes, then for small E and M this coincidence factor can be written as

$$\Gamma = 1 - \frac{E + M}{2}$$

To perform these measures between the aEIF model and the detailed model, they first calibrated all the parameter values using several systematic procedures, which we will specify later in this project, and then they used the same simulation method for both models.

In a first instance, they tested random conductance injection, for which the voltage behave in almost exactly the same way, and most of the spikes were not missed. Averaged between several different conductances, the aEIF model emitted 3% more spikes and missed 4% of the spikes generated by the detailed model, which gives a coincidence factor of 96%. As far as subthreshold dynamics go, they are indistinguishable between the two models, but when a step current is applied, a shift between the two spike trains appears after the first spike, and it grows with time.

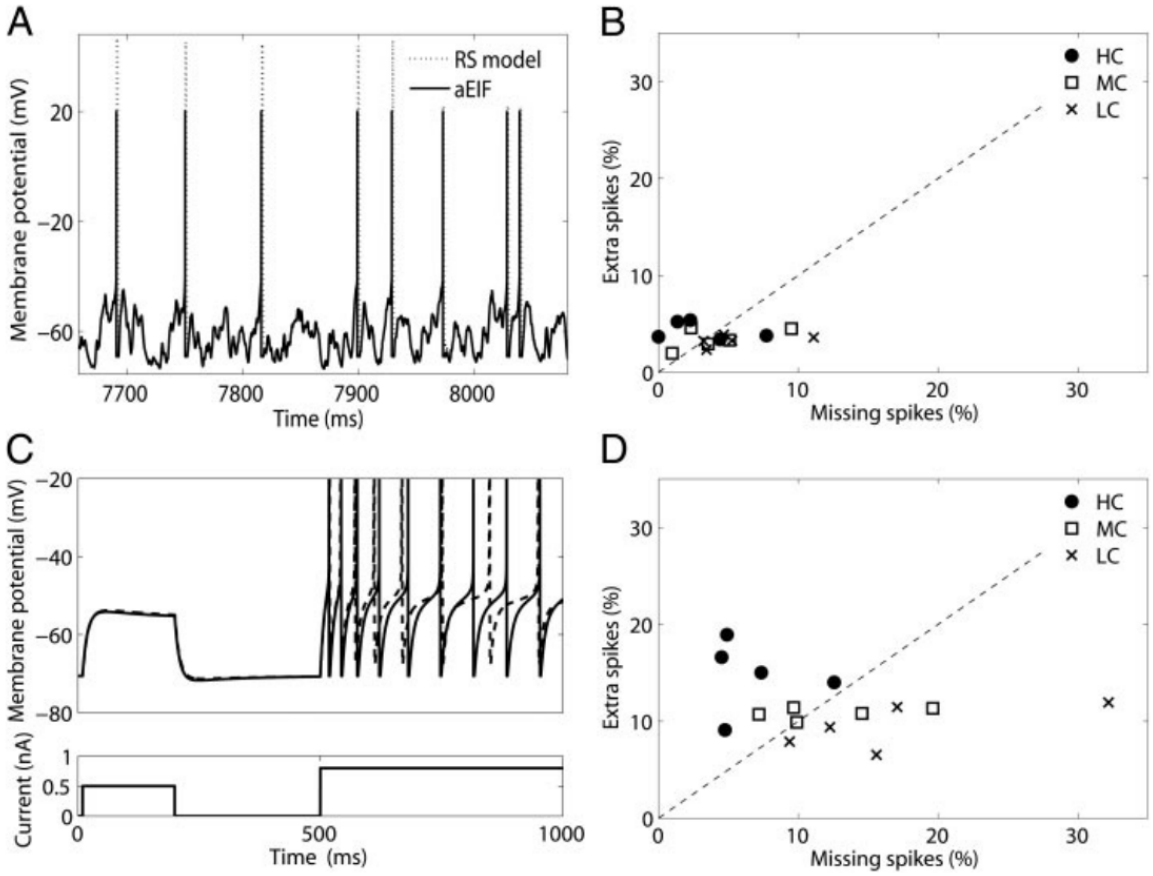

Figure 1: A: Regular spiking behavior of V in the two models. B: M and E values for different conductance levels in regular spiking. C: Step-current induced spike trains in both models. D: M and E values for different conductance levels in spike trains behavior.

In a first instance, they tested random conductance injection, for which the voltage behave in almost exactly the same way, and most of the spikes were not missed, which we can see in Figure 1A and 1B. Averaged between several different conductances,

the aEIF model emitted 3% more spikes and missed 4% of the spikes generated by the detailed model, which gives a coincidence factor of 96%. As far as subthreshold dynamics go, they are indistinguishable between the two models, but when a step current is applied, a shift between the two spike trains appears after the first spike, and it grows with time, which we can see in Figure 1C.

3 Subthreshold dynamics

To study analytically the properties of this model, it is useful to perform a linear coordinate transformation to write the differential equations in a simpler way. We'll use the transformation used in Touboul and Brette (2008)[5], which is

$$\begin{aligned}
\tau_w' &= \frac{\tau_w}{\tau_m} = \frac{g_L \tau_w}{C} \\
a' &= \frac{a}{g_L} \\
I' &= \frac{I}{g_L \Delta_T} + \left(1 + \frac{a}{g_L}\right) \frac{E_L - V_T}{\Delta_T} \\
t' &= \frac{t}{\tau_m} \\
b' &= \frac{b}{g_L \Delta_T} \\
V_r' &= \frac{V_r - V_T}{\Delta_T} \\
V'(t') &= \frac{V(t) - V_T}{\Delta_T} \\
w'(r') &= \frac{w(t) + a\left(E_L - V_T\right)}{g_L \Delta_T}
\end{aligned}$$

In these new coordinates and constants, the systems becomes:

$$\begin{cases} \dot{V'} & = -V' + e^{V'} - w' + I' \\ \tau_w' \dot{w'} & = a' V' - w' \end{cases}$$

3.1 Fixed points curve

To obtain curves of fixed points, we must set the derivatives of the system to 0, which entails

$$\begin{aligned}
&\begin{cases} 0 & = -V' + e^{V'} - w' + I' \\ 0 & = a' V' - w' \end{cases} \\
\Longrightarrow &\begin{cases} e^{V'} - \left(a' + 1\right) V' & = -I' \\ w' & = a' V' \end{cases}
\end{aligned} \tag{4}$$

The appearance of the nullclines for the aEIF model is represented in the following figure.

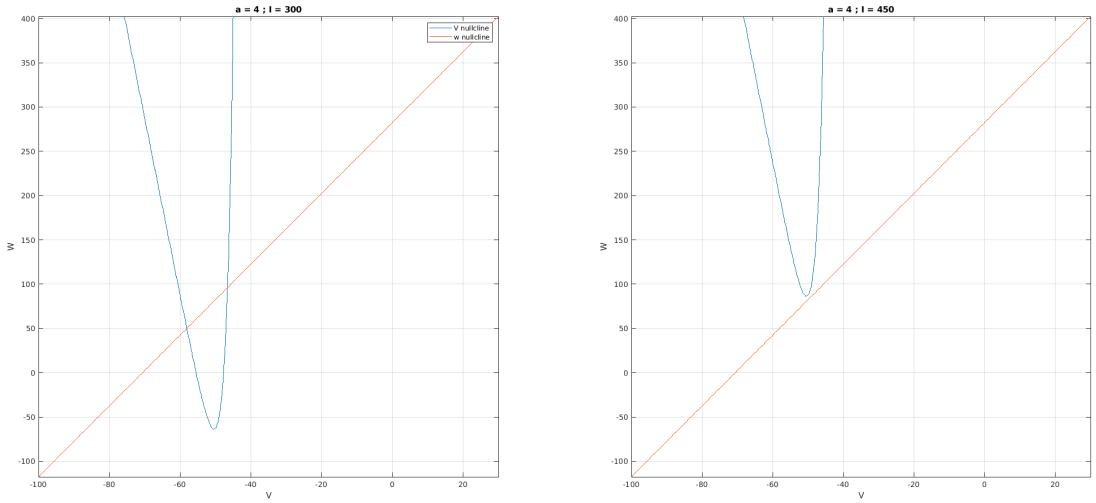

Figure 2: V and w Nullclines.

Considering the fixed point expression, let's define $F(V') = e^{V'} - (a'+1)V'$. Because $F''(V') = e^{V'} > 0 \; \forall V'$, F is convex, which implies it has a minimum at a certain $V'_{\min}$, which in this case is $F'(V'_{\min}) = 0 \implies V'_{\min} = \log(1+a')$. Thus, we can split the existence of solution to the fixed point equation in 3 cases: if $F(V'_{\min}) > -I'$, then there are no V' solutions, if $F(V'_{\min}) = -I'$, there is only the solution $V' = V'_{\min}$, and if $F(V'_{\min}) < -I'$ there are two solutions, let's call them V_+ and V_-.

To write (4) in the form $V_{\text{fixed}}(I)$, we can use Lambert's W function. The equation

$$ye^y = x \tag{5}$$

has solutions

$$y = \begin{cases} W_0(x) & \text{, if } x \geq 0 \\ W_0(x) \text{ and } W_{-1}(x) & \text{, if } -\frac{1}{e} \leq x < 0 \end{cases}$$

We can transform (4) in the form of (5), by the following procedure:

$$\begin{aligned} (a'+1)V' - I' &= e^{V'} \\ [(a'+1)V' - I']e^{-V'} &= 1 \\ \left[-V' + \frac{I'}{(1+a')}\right] e^{-V'} e^{\frac{I}{(1+a')}} &= -\frac{1}{(1+a')} e^{\frac{I}{(1+a')}} \\ \left[-V' + \frac{I'}{(1+a')}\right] e^{\left[-V' + \frac{I'}{(1+a')}\right]} &= -\frac{1}{(1+a')} e^{\frac{I}{(1+a')}} \end{aligned}$$

Thus, the solutions are:

$$\begin{cases} V'_+ &= -\frac{I'}{(1+a')} - W_0\left[-\frac{1}{(1+a')}e^{\frac{I}{(1+a')}}\right] \\ V'_- &= -\frac{I'}{(1+a')} - W_{-1}\left[-\frac{1}{(1+a')}e^{\frac{I}{(1+a')}}\right] \end{cases}$$

$$\iff \begin{cases} V_+ &= E_L + \frac{I}{g_L+a} - \Delta_T W_0\left(-\frac{1}{1+a/g_L}e^{\frac{I}{\Delta_T(g_L+a)}} + \frac{E_L-V_T}{\Delta_T}\right) \\ V_- &= E_L + \frac{I}{g_L+a} - \Delta_T W_{-1}\left(-\frac{1}{1+a/g_L}e^{\frac{I}{\Delta_T(g_L+a)}} + \frac{E_L-V_T}{\Delta_T}\right) \end{cases}$$

These branches are represented in the following figure.

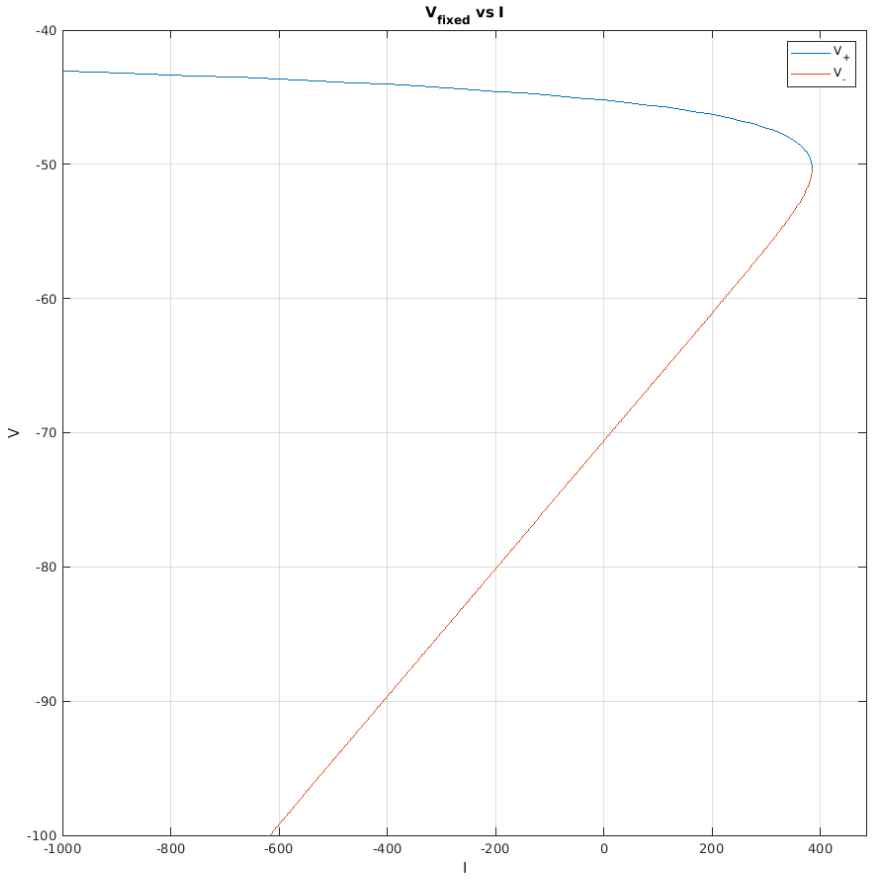

Figure 3: V and w Nullclines.

3.2 Stability of fixed points

To analyze if a fixed point is stable, we need to analyze the determinant Δ and the trace τ of the Jacobian matrix $\mathbf{J}'(V', w')$ at those points. For our model, we have:

$$\mathbf{J}'(V', w') = \begin{bmatrix} \frac{\partial \dot{V}'}{\partial V'} & \frac{\partial \dot{V}'}{\partial w'} \\ \frac{\partial \dot{w}'}{\partial V'} & \frac{\partial \dot{w}'}{\partial w'} \end{bmatrix} = \begin{bmatrix} e^{V'} - 1 & -1 \\ \frac{a'}{\tau'_w} & -\frac{1}{\tau'_w} \end{bmatrix}$$

which gives a determinant of

$$\begin{aligned} \Delta &= -\frac{e^{V'} - 1}{\tau'_w} + \frac{a'}{\tau'_w} \\ &= -\frac{e^{V'}}{\tau'_w} + \frac{1}{\tau'_w}(1 + a') \end{aligned}$$

Now, this function is monotonically decreasing, since

$$\frac{d\Delta}{dV'} = -\frac{e^{V'}}{\tau'_w} < 0 \ \forall V'$$

and it's zeros is $\Delta = 0 \implies V^* = \log(1 + a') = V'_{\min}$. Since it is always decreasing, for all $V' > V'_{\min}$, i.e. for all the values in the V'_+ branch, we have that $\Delta < 0$, which means they are all saddle points, i.e. they are unstable fixed points.

Because we also have that $\Delta > 0$ for all $V' < V'_{\min}$, in order to analyze their stability we need to study the behavior of the trace $\tau = \mathrm{T}(\mathbf{J}'(V', w'))$. It's value is

$$\tau = e^{V'} - 1 - \frac{1}{\tau'_w}$$

Analyzing τ at the branch V'_-, we can use the fact that τ is an increasing function of V', and $V'_- < V'_{\min} < V'_+$, which implies:

$$\tau\left(V'_-\right) \leq \tau\left(V'_{\min}\right) = a' - \frac{1}{\tau'_w}$$

Now, let's denominate $a' < \frac{1}{\tau'_w}$ by case I and $a' > \frac{1}{\tau'_w}$ by case II.

Thus, in case I, we have have that

$$a' < \frac{1}{\tau'_w} \implies \tau(V') < 0 \ \forall V' \in \left\{V'_-\right\}$$

i.e. the entire V'_- is stable. In case II, there might be solutions of V' s.t. $\tau(V') > 0$, as we will see.

3.3 Case I - $a < \frac{C}{\tau_w}$

As it was argued before, when $a' < \frac{1}{\tau'_w} \iff a < \frac{C}{\tau_w}$, the entire V'_- branch is stable, which implies that two stable and unstable fixed points $\left(V'_+ \text{ and } V'_-\right)$ merge at $V'_{\min}$ and disappear, i.e. this is a saddle node bifurcation. The current at which this bifurcation happens is, which we'll denote by I_{rh}, which stands for rheobase current, the minimum constant current required to

elicit a spike, i.e. the first point at which the stable point becomes unstable.

$$
\begin{aligned}
I'_{rh} &= -e^{V'_{\min}} + (a'+1)\, V'_{\min} \\
&= -(1+a') + (1+a')\log(1+a') \\
\implies \frac{I^I_{rh}}{g_L \Delta_T} + \left(1+\frac{a}{g_L}\right)\frac{E_L - V_T}{\Delta_T} &= -\left(1+\frac{a}{g_L}\right) + \left(1+\frac{a}{g_L}\right)\log\left(1+\frac{a}{g_L}\right) \\
I^I_{\text{th}} &= (g_L + a)\left[V_T - E_L - \Delta_T + \Delta_T \log\left(1+\frac{a}{g_L}\right)\right]
\end{aligned}
$$

For the constants (3), $\frac{C}{\tau_w} \approx 1.9514$. Thus, picking $a = 1$, we have the following saddle-node bifurcation plot:

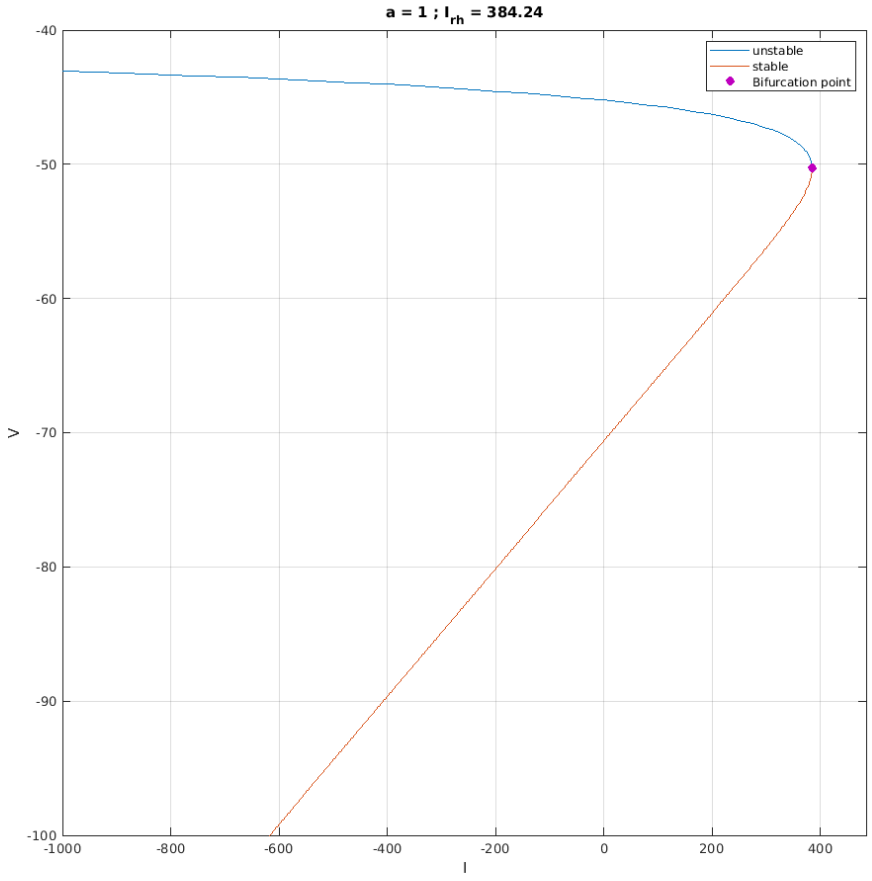

Figure 4: Saddle-node bifurcation plot.

3.4 Case II - $a > \frac{C}{\tau_w}$

For case II, $a' > \frac{1}{\tau'_w}$, the trace τ may have positive values in the V_- brach generally, and the solutions to $\tau = 0$ are:

$$
V'_{rh} = \log\left(1 + \frac{1}{\tau'_w}\right)
$$

Thus, because $V'_{rh} < V'_{\min}$, the initially stable point in the branch V'_{-} becomes unstable before the merging of the two branches, and so it corresponds to an Andronov-Hopf bifurcation. The current at which it happens is

$$
\begin{aligned}
I'_{rh} &= -e^{V'_{rh}} + (a'+1)\, V'_{rh} \\
&= -\left(1+\frac{1}{\tau'_w}\right) + \left(1+\frac{a}{g_L}\right)\log\left(1+\frac{1}{\tau'_w}\right) \\
\frac{I^{II}_{rh}}{g_L \Delta_T} + \left(1+\frac{a}{g_L}\right)\frac{E_L - V_T}{\Delta_T} &= -\left(1+\frac{C}{g_L \tau_w}\right) + \left(1+\frac{a}{g_L}\right)\log\left(1+\frac{C}{g_L \tau_w}\right) \\
I^{II}_{\mathrm{rh}} &= (g_L + a)\left[V_T - E_L - \Delta_T + \Delta_T \log\left(1+\frac{\tau_m}{\tau_w}\right)\right] + \Delta_T\left(a - \frac{C}{\tau_w}\right)
\end{aligned}
$$

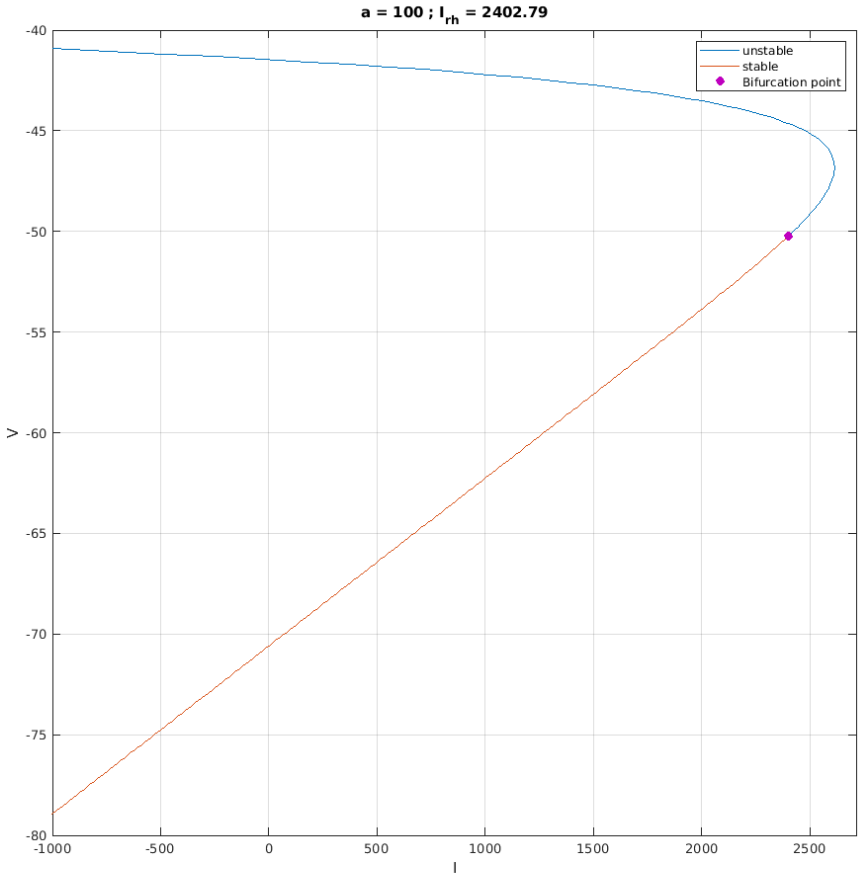

Figure 5: Andronov-Hopf bifurcation plot.

3.5 Oscillations

The system will oscillate around a fixed point V' if and only if the imaginary part of the eigenvalues of the Jacobian matrix is non-null at V'. The discriminant δ of the system is:

$$\begin{aligned}
\delta = \tau^2 - 4\Delta &= \left[e^{V'} - 1 - \frac{1}{\tau'_w}\right]^2 - 4\left[-\frac{e^{V'}-1}{\tau'_w} + \frac{a'}{\tau'_w}\right] \\
&= \left(e^{V'} - 1\right)^2 - 2\frac{e^{V'}-1}{\tau'_w} + 4\frac{e^{V'}-1}{\tau'_w} + \frac{1}{\left(\tau'_w\right)^2} - \frac{4a'}{\tau'_w} \\
&= \left(e^{V'} - 1\right)^2 + 2\frac{e^{V'}-1}{\tau'_w} + \frac{1}{\left(\tau'_w\right)^2} - \frac{4a'}{\tau'_w} \\
&= \left[e^{V'} - 1 + \frac{1}{\tau'_w}\right]^2 - \frac{4a'}{\tau'_w}
\end{aligned}$$

Thus, to have oscillatory behavior around a stable point V'_*, we need

$$\left[e^{V'_*} - 1 + \frac{1}{\tau'_w}\right]^2 - \frac{4a'}{\tau'_w} < 0$$

Thus, we are looking for solutions to the equation

$$\begin{aligned}
e^{V'_*} - 1 + \frac{1}{\tau'_w} &= \pm 2\sqrt{\frac{a'}{\tau'_w}} \\
\left(e^{V'_*}\right)_{\pm} &= 1 - \frac{1}{\tau'_w} \pm 2\sqrt{\frac{a'}{\tau'_w}}
\end{aligned}$$

As we've seen before, only points along the branch V_- are prone to be stable, and they satisfy $V_- < \log\left(1 + a'\right)$, thus there exist solutions to the expression above along the branch V_- if and only if $0 < e^{V'_*} \leq 1 + a'$. Let's consider the $\left(e^{V'_*}\right)_+$ expression first. We have:

$$\begin{aligned}
\frac{\tau'_w - 1 + 2\sqrt{a'\tau'_w}}{\tau'_w} &\leq 1 + a' \\
\iff \tau'_w - 1 + 2\sqrt{a'\tau'_w} - \tau'_w - a'\tau'_w &\leq 0 \\
\iff 1 - 2\sqrt{a'\tau'_w} + a'\tau'_w &\geq 0 \\
\iff \left(1 - \sqrt{a'\tau'_w}\right)^2 &\geq 0
\end{aligned}$$

The last equation is always true. Now we need to check where $\left(e^{V'_*}\right)_+ > 0$:

$$\begin{aligned}
&\frac{\tau'_w - 1 + 2\sqrt{a'\tau'_w}}{\tau'_w} > 0 \\
\iff\ &\tau'_w - 1 + 2\sqrt{a'\tau'_w} > 0 \\
\iff\ &2\sqrt{a'\tau'_w} > 1 - \tau'_w \\
\iff\ &a' > \frac{1}{4\tau'_w}\left(1-\tau'_w\right)^2
\end{aligned}$$

From the second line, we can see that $\left(e^{V'_*}\right)_+ > 0$ is satisfied already if $\tau'_w > 1$, but if $\tau'_w < 1$ it is still satisfied if $a' > \frac{1}{4\tau'_w}\left(1-\tau'_w\right)^2$. Analogously, solutions to $\left(e^{V'_*}\right)_- = 1 - \frac{1}{\tau'_w} - 2\sqrt{\frac{a'}{\tau'_w}}$ exist when $\tau'_w > 1$ and $a' \leq \frac{1}{4\tau'_w}\left(1-\tau'_w\right)^2$. The currents of these critical points are

$$\begin{aligned}
I'_\pm &= \left(1+a'\right)V'_* - e^{V'_*} \\
&= \left(1+a'\right)\log\left[1 - \frac{1}{\tau'_w} \pm 2\sqrt{\frac{a'}{\tau'_w}}\right] - 1 - \frac{1}{\tau'_w} - 2\sqrt{\frac{a'}{\tau'_w}}
\end{aligned}$$

which corresponds to

$$I_\pm = \left(g_L + a\right)\Delta_T \log\left(\frac{g_L\tau_w - C \pm 2\sqrt{aC\tau_w}}{g_L\tau_w}\right) - \Delta_T\frac{g_L\tau_w - C \pm 2\sqrt{aC\tau_w}}{\tau_w} - \left(g_L+a\right)\left(E_L - V_T\right)$$

Thus, to summarize we have that when $\tau'_w < 1$ oscillations around equilibria exist when $a' > \frac{1}{4\tau'_w}\left(1-\tau'_w\right)^2$ and $I' < I'_+$, and when $\tau'_w > 1$ they exist when $a' < \frac{1}{4\tau'_w}\left(1-\tau'_w\right)^2$ for any $I'_{\min} < I' < I'_{\max}$ and when $a' > \frac{1}{4\tau'_w}\left(1-\tau'_w\right)^2$ for any $I' < I'_+$.

4 Parameter fitting

A real advantage of having a simple two dimensional model is that systematic procedures to extract parameters from experimental data to fit them to the model are much easier to come up with, whereas they are mostly unknown for complicated models that capture behavior of neurons in detail, like the Hodgkin-Huxley model. In our reference paper [1] it's shown that all parameters can be systematically extracted using a series of standard simulation paradigms, which we'll go through now.

The membrane capacitance C, the leak conductance g_L and the leak reversal potential E_L can be determined by performing an exponential fit to the V plot generated by the reference model when inducting a current pulse.

To determine the subthreshold adaptation constant a, we first note that far away from the potential threshold V_T, the term $\mathrm{e}^{(V-V_\mathrm{T})/\Delta_\mathrm{T}}$ can be neglected. We can make the system converge to the stable node V_-, and if the current I is slowly increased such that the system is always in that stable node, then $\dot{V}$ can be neglected, which by (1) implies

$$I = (g_L + a)(V - E_L)$$

Thus, we can determine a by performing a linear fit to the $I(V)$ plot obtain from the detailed model.

To determine the spike-triggered adaptation b, the procedure can be: first, depolarize the membrane potential close to the average potential during synaptic stimulation, and then inject short but strong current pulses in order to trigger spikes. Just before the pulse onset, the potential is till far away from the threshold potential, and thus we can neglect the exponential term again, which implies

$$w = -C\frac{dV}{dt} - g_{\mathrm{L}}(V - E_{\mathrm{L}}) + I$$

The differences from the successive w's obtained in this way, for each spike, and the contribution from the subthreshold adaptation a gives the contribution to spike-triggered adaptation b. The fitting of these values to an exponential enables the estimate of b and τ_w.

In order to determine Δ_T and V_T, we can proceed as follows: For each value of Δ_T, choose V_T such that our model and the detailed model have the same average firing rate (*effective threshold*). Then, they chose the Δ_T valued that minimized the variance of V_T.

5 Conclusion

In this project, we've seen that the Adaptive Integrate-and-Fire model can be well fitted to reproduce neuronal behavior as modeled by much complicated models, and exploited its simplicity to determine analytically regions of different behaviors depending on the parameters I, a and C.

References

[1] Wulfram Gerstner and Romain Brette. Adaptive exponential integrate-and-fire model as an effective description of neuronal activity. *Journal of Neurophysiology*, 94, 2005.

[2] Werner Kistler, Wulfram Gerstner, and Leo van Hemmen. Reduction of the hodgkin-huxley equations to a single-variable threshold model. *Neural Computation*, 9, 2000.

[3] DA McCormick, Z Wang, and J. Huguenard. Neurotransmitter control of neocortical neuronal activity and excitability. *Cereb Cortex*, 3, 1993.

[4] Jonathan Touboul. Bifurcation analysis of a general class of nonlinear integrate-and-fire neurons. *SIAM Journal of Applied Mathematics*, 68:1045–1079, 2008.

[5] Jonathan Touboul and Romain Brette. Dynamics and bifurcations of the adaptive exponential integrate-and-fire model. *Biological Cybernetics*, 99, 2008.